Assessment of the 2022 Hunga-Tonga Volcanic Eruption's Impact on the Ionosphere in the Chinese Region through Tomography

Yun Sui(1), Haiyang Fu*(1), Feng Xu(1), Denghui Wang (2), Shaojun Feng(2) and Yaqiu Jin(1)
(1) Key Laboratory for Information Science of Electromagnetic Waves (MoE), Fudan University, Shanghai, China
(2) Qianxun Spatial Intelligence Inc., Shanghai, China

Abstract

Ionospheric electron density monitoring is of great significance for positioning and navigation, communication technology and space weather research. To alleviate the ill-posed problem of ionospheric electron density inversion caused by sparse and unevenly distributed stations, the DCS-PCA (Dynamic Compressive Sensing-Principal Component Analysis) ionospheric tomography method is used in the paper. This method is a real-time data-driven tomographic method based on compressive sensing and fusion of measurement data. This paper focuses on investigating the influence of the 2022 Hunga-Tonga volcanic eruption on the ionosphere in the Chinese region. The GPS navigation observations were collected from 130 stations within the Qianxun Ground-Based Augmentation System. The constructed ionospheric electron density model demonstrates the DCS-PCA method's ability to capture the spatiotemporal evolution of the ionosphere during the volcanic eruption. In the ionospheric tomography model, equatorial plasma bubbles were observed in East and Southeast Asia following volcanic waves, leading to reduced electron density, consistent with the reference. The ionospheric tomographic model in this study possesses quasi-real-time capability, high efficiency, and sparse station adaptability, providing a new tomographic solution for ionospheric monitoring.

1 Introduction

The ionosphere constitutes a significant source of error in radio propagation, impacting various applications such as communication, navigation, and positioning. The advent of GNSS (Global Navigation Satellite System) big data networks has led to the development of ionospheric models based on GNSS data, serving as a vital tool for ionospheric monitoring. Although the Vertical Total Electron Content (VTEC) ionospheric model, relying on the thin-shell assumption, has gained widespread adoption, it fails to capture the three-dimensional spatiotemporal variations of the ionosphere. With advancements in observation techniques and computer technology, ionospheric models have evolved from the initial two-dimensional VTEC model to encompass multi-layer VTEC models and three-dimensional electron density models. In the present, the advancement extends to real-time four-dimensional electron density models, offering a more comprehensive representation of ionospheric behavior. It is of great significance for studying the spatiotemporal characteristics and monitoring abnormal features of the ionosphere.

Computerized Ionospheric Tomography (CIT), proposed by Austen in 1986, is a technique for inverting the electron density distribution in the ionosphere based on the Slant Total Electron Content (STEC) along satellite-to-ground station paths(1; 2; 3; 4; 5; 6). The sparsity and uneven distribution of actual observation sites in the tomographic process lead to an ill-posed problem. To mitigate the ill-posed nature of the problem, many tomographic methods assume that the ionosphere remains constant over an extended period, collecting enough observations for tomographic analysis. However, this assumption contradicts the real-time spatiotemporal variations of the ionosphere. The compressive sensing fusion data-driven regional tomography method, known as the CS-PCA (Compressive Sensing-Principal Component Analysis) method, was introduced to address the ill-posed problem in paper (7). Through the integration of feature extraction from the ionospheric model and real-time navigation observations, high-precision ionospheric tomography based on sparse observations was achieved. Subsequently, the DCS-PCA (Dynamic Compressive Sensing-Principal Component Analysis) regional ionospheric tomography model, driven by dynamic measured tomographic data, was proposed in paper (8).

Volcanic eruptions have the potential to induce perturbations in both the Earth's background atmosphere and ionosphere, rendering them subjects of paramount significance within the domain of space weather research. In order to investigate the impact of the 2022 Hunga-Tonga volcanic eruption on the ionosphere in the Chinese region, we constructed the ionospheric tomography model on the day of the event using GPS observations collected from the Qianxun Ground-Based Augmentation System. The study examines the influence of the eruption on the spatiotemporal evolution of the ionosphere.

2 Regional Ionospheric Tomography Method

Utilizing the GNSS dual-frequency pseudo-range P and carrier phase L signals received from the IGS Ground-based System, this study employs the un-differenced and un-combined precise point positioning (UCPPP) method, which incorporates known fixed station coordinates, to derive ionospheric delay data (10):

$$I(x^S, x_R, t)' = \frac{40.3 \cdot STEC}{f_1^2} + \frac{f_2^2}{f_1^2 - f_2^2} DCB_R - \frac{f_2^2}{f_1^2 - f_2^2} DCB^S \quad (1)$$

where x^S and x_R are the coordinate of the satellite S and the receiver R, t is the time corresponding to the observation; DCB_R is the bias of receiver and DCB^S is the bias of satellite. f_1 and f_2 are the operating frequency of navigation signal.

The STEC from the satellite S to the receiver R is defined as the integral of the electron density $\mathbf{N}_e$ along the signal path, $STEC(x^S, x_R, t) = \int_R^S \mathbf{N}_e dl$. To achieve accurate STEC measurements, it is essential to address biases introduced by receiver and satellite. This is accomplished through the application of the differential STEC (dSTEC) method to mitigate receiver biases, and the utilization of external products to correct satellite biases. The grid-based tomography method divides the inversion region into three-dimensional grids, and the electron density in each grid is evenly distributed:

$$\mathbf{dSTEC_{m\times 1}} = \Phi_{m\times n} \cdot \mathbf{N_e}_{n\times 1} + \varepsilon_{m\times 1} \quad (2)$$

where $\mathbf{d}STEC_{m\times 1}$ is the differential STEC vector, and m is the total number of rays; $\Phi_{m\times n}$ is the differential design matrix composed of the intercept of GNSS ray in each grid $d_{i,j}$, $i = 1, ..., m$, $j = 1, ..., n$; n is the total number of grids; $\mathbf{N_e}_{n\times 1}$ is the electron density vector; $\varepsilon_{m\times 1}$ is the error vector related to observation noise and system noise.

The DCS-PCA (Dynamic Compressive Sensing-Principal Component Analysis) method is used in this paper. This approach relies on dynamic measured tomographic data. Unlike conventional methods that directly estimate the signal in its native domain, this approach emphasizes the estimation of the sparse signal in the transformed domain.

$$\mathbf{N_e}_{n\times 1} = \sum_{i=1}^{K} \Psi_i \cdot \mathbf{w}_i \quad (3)$$

where $\mathbf{w}$ is $K \times 1$ dimension sparse vector. Ψ is $n \times K$ dimension projection matrix, which representing the ionospheric characteristics from the prior matrix $\mathbf{X}$. The real-time electron density reconstruction results are used to dynamically modify the prior matrix $\mathbf{X}$ in this paper, ensuring that the projection matrix Ψ extracted by the data-driven approach aligns with the actual ionospheric characteristics.

The cost function for the ionospheric tomography method takes the sum of the L_2 norm term representing the reconstruction error and L_1 norm term representing the sparsity. L_1 norm regularization term is introduced to constrain the solutions for $\mathbf{w}$ to be sparse.

$$Loss = \text{argmin}_{\mathbf{w}} \left\{ \|\mathbf{dSTEC}^c - \Phi^c \cdot \Psi \cdot \mathbf{w}\|_2^2 + \lambda_{cs} \cdot \|\mathbf{w}\|_1 \right\} \quad (4)$$

where $\mathbf{w}$ is the sparse signal to be solved, $\mathbf{dSTEC}^c$ is the inter satellite differential STEC with constraints, Φ^c is the differential design with constraints, $\mathbf{w}$ is the sparse signal in the transformation domain to be solved, Ψ is the projection matrix, λ_{cs} is the hyper-parameter used to control the proportion of error term and sparse term in the cost function.

3 Data and Results

In this study, we investigate the impact of the eruption of the Hunga-Tonga volcano, located at latitude 20.32°S and longitude 174.24°E, on the ionosphere in the Chinese region. This volcanic eruption occurred on January 15, 2022, at UTC 04:14 and is considered the most significant eruption of the past three decades. It caused substantial disruptions to the customary cyclic behaviors of the ionosphere. Chinese regional ionospheric tomography is being studied during the Hunga-Tonga volcano eruption. The GPS data utilized in this study were collected from 130 stations within the Qianxun Ground-Based Augmentation System. These data include the basic GPS dual-frequency code and carrier phase observations, with a recording interval of 30 seconds. An elevation mask of 30° is used to reduce multi-path effects. The three-dimensional ionospheric model range from 68° to 138° in terms of longitude direction and from 14° to 61° in terms of latitude direction. The spatial resolution is 2.5° and 2.5° in longitude and latitude direction, respectively. The altitudes ranging from 100 to 1,000 km with a resolution of 50 km and then up to 1,300 km with a resolution of 100 km. The temporal resolution of the model is 5 minutes.

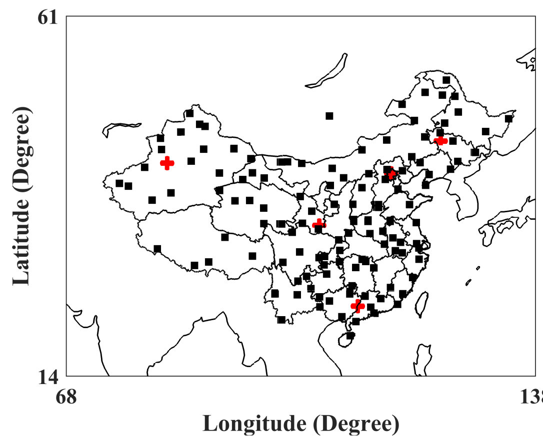

Figure 1. GNSS receiver locations used in the tomographic reconstruction. Black dots represent the stations used for modeling, while the red dots represent independent reference stations used for validating model performance.

Based on actual GPS observation data on January 15, 2022

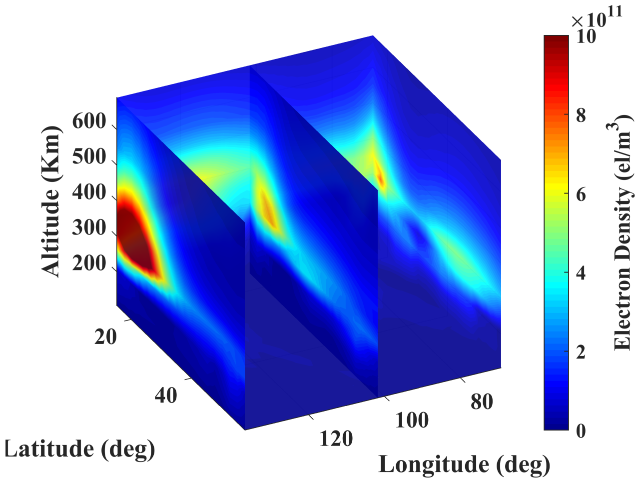

(a) UTC 11:30

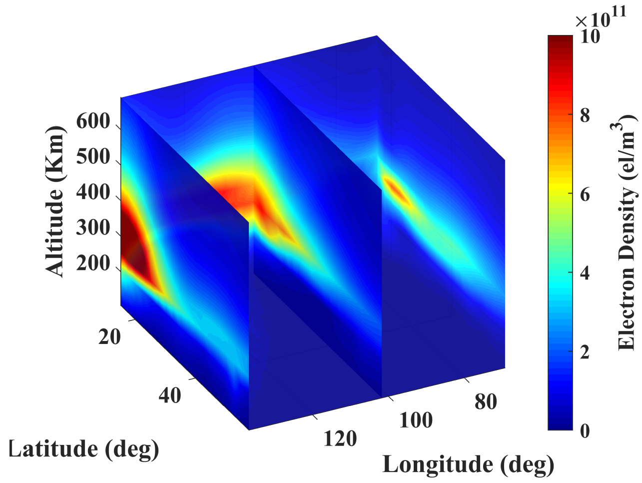

(b) UTC 12:30

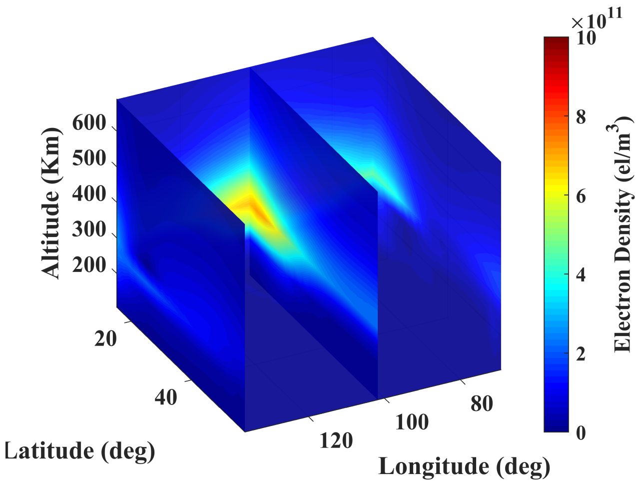

(c) UTC 13:30

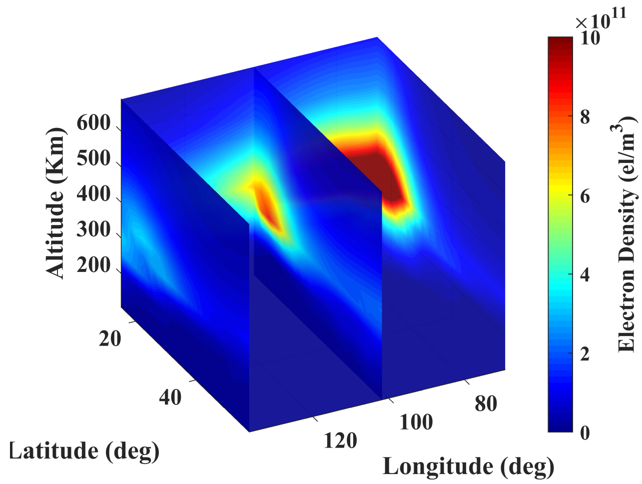

(d) UTC 14:30

Figure 2. The reconstructed three-dimensional electron density distribution in China region based on real GPS observation on January 15, 2022.

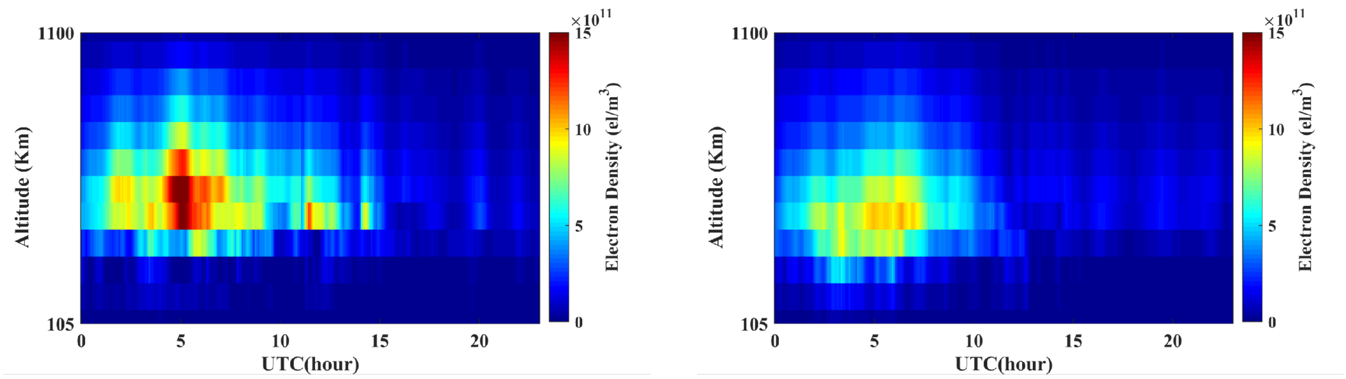

Figure 3. Comparison between the electron density of the Sanya station (18°N, 109°E) and the Beijing station (40°N, 116°E) over different epoch based on real GPS observation on January 15, 2022.

obtained from ground-based stations, the ionospheric electron density model for the Chinese region is constructed using the regional DCS-PCA tomography method. Figure 2 presents the three-dimensional electron density distribution in the Chinese region from UTC 11:30 to UTC 14:30 on January 15, 2022. As sunset occurred, it was observed that significant equatorial plasma bubbles consistently appeared in the East Asia and Southeast Asia sector following the arrival of volcanic-triggered waves, resulting in a substantial reduction in electron density. Equatorial plasma bubbles are a phenomenon of plasma density depletion with small-scale density irregularities, normally observed in the equatorial ionosphere. In line with the findings reported in Reference (9), this equatorial plasma bubbles phenomenon was observed in the Asia-Pacific region after the largest-on-record January 15, 2022 eruption of the Tonga volcano.

Figure 3 illustrates the electron density evolution with respect to altitude and time at two distinct latitude coordinates: the Sanya station (18°N, 109°E) and the Beijing station (40°N, 116°E). It can be observed that Sanya is notably affected by the equatorial plasma bubbles induced by the volcano, leading to electron density depletion at an altitude of 450 km between UTC 10:00 and UTC 15:00. However, it can be seen that Beijing, located at a latitude of 40 degrees, is no longer influenced by the equatorial plasma bubbles, and thus, there is no significant electron density depletion.

4 Conclusion and Discussion

This paper develops a ionospheric tomography model based on DCS-PCA and applies it to the 2022 Hunga-Tonga volcanic eruption event. Using GPS data from 130 stations within the Qianxun Ground-Based Augmentation System, a regional ionospheric tomographic model is constructed using a measurement-driven compressed sensing sparse imaging method. The results show that the DCS-PCA method can capture the temporal evolution of tomographic electron density. Equatorial plasma bubbles observed in East and Southeast Asia after volcanic waves reduced electron density, in line with the reference. Therefore, the proposed method plays an important role in ionospheric monitoring and high-precision positioning in active ionospheric regions.

5 Acknowledgements

The authors are supported by the National Key Research and Development Program of China (2021YFA0717300). Yun Sui is supported by the China Postdoctoral Science Foundation (GZC20230462) and Shanghai Super Postdoctoral Funding Program.

References

[1] J. R. Austen, S. J. Franke, and C. H. Liu,"Ionospheric imaging using computerized tomography," Radio Science, 23, 3, May/Jun 1988, pp. 299–307.

[2] J. M. Juan, A. Rius, M. Hernández-Pajares, and J. Sanz, "A two-layer model of the ionosphere using global positioning system data," *Geophysical Research Letters*, **24**, 393–396, 1997.

[3] M. Hernández-Pajares, J. M. Juan, J. Sanz, and J. G. Solé, "Global observation of the ionospheric electronic response to solar events using ground and LEO GPS data," *Journal of Geophysical Research*, **103**, 20789–20796, 1998.

[4] R. Garcia, and F. Crespon, "Radio tomography of the ionosphere: Analysis of an underdetermined, ill-posed inverse problem, and regional application." Radio Science, 43, 2, 2008, pp. 1–13.

[5] G. K. Seemala, M. Yamamoto, A. Saito, and C.-H. Chen, "Three dimensional GPS ionospheric tomography over Japan using constrained least squares," J. Geophys. Res. Space Phys., vol. 119, no. 4, pp. 3044–3052, Apr. 2014.

[6] G. S. Bust and C. N. Mitchell, "History, current state, and future directions of ionospheric imaging." Reviews of Geophysics, 46, 1, 2008.

[7] Y. Sui, et al., "Sparse reconstruction of 3-D regional ionospheric tomography using data from a network of GNSS reference stations." IEEE Transactions on Geoscience and Remote Sensing, 60, 2021, pp. 1–15.

[8] Y. Sui, H. Fu, F. Xu, D. Wang, S. Feng and Y. Jin, "Ionospheric Tomography Model Driven by Dynamic Measured Data and Its Multi-GNSS Verification," 2023 XXXVth General Assembly and Scientific Symposium of the International Union of Radio Science (URSI GASS), Sapporo, Japan, 2023, pp. 1-4, doi: 10.23919/URSIGASS57860.2023.10265311.

[9] A. Shinbori, T. Sori, Y. Otsuka, M. Nishioka, S. Perwitasari, T. Tsuda, A. Kumamoto, F. Tsuchiya, S. Matsuda, Y. Kasahara, A. Matsuoka, S. Nakamura, Y. Miyoshi, and I. Shinohara, "Generation of equatorial plasma bubble after the 2022 Tonga volcanic eruption," Scientific Reports, vol. 13, 2023, doi: 10.1038/s41598-023-33603-3.

[10] J. F. Zumberge, M. B. Heftin, D. C. Jefferson, and M. M. Watkins, "Precise point positioning for the efficient and robust analysis of GPS data from large networks," Journal of Geophysical Research Solid Earth, 102, 1, 1997, pp. 5005—5017.